Biosensors and Bioelectronics 36 (2012) 222–229

Contents lists available at SciVerse ScienceDirect

Biosensors and Bioelectronics

journal homepage: www.elsevier.com/locate/bios

Quantification of surface etching by common buffers and implications on the accuracy of label-free biological assays

Sunmin Ahn [a], Philipp S. Spuhler [a], Marcella Chiari [b], Mario Cabodi [a], M. Selim Ünlü [a,c,*]

[a] Department of Biomedical Engineering, Boston University, Boston, MA, USA
[b] Consiglio Nazionale delle Ricerche, Istituto di Chimica del Riconoscimento Molecolare, Milano, Italy
[c] Department of Electrical and Computer Engineering, Boston University, Boston, MA, USA

ARTICLE INFO

Article history:
Received 13 March 2012
Accepted 11 April 2012
Available online 21 April 2012

Keywords:
DNA microarrays
Proteins microarrays
Label-free detection
Optical interferometry
Glass stability
Buffer effect

ABSTRACT

High throughput analyses in biochemical assays are gaining popularity in the post-genomic era. Multiple label-free detection methods are especially of interest, as they allow quantitative monitoring of biomolecular interactions. It is assumed that the sensor surface is stable to the surrounding medium while the biochemical processes are taking place. Using the Interferometric Reflectance Imaging Sensor (IRIS), we found that buffers commonly used in biochemical reactions can remove silicon dioxide, a material frequently used as the solid support in the microarray industry. Here, we report 53 pm to 731 pm etching of the surface silicon oxide over a 12-h period for several different buffers, including various concentrations of SSC, SSPE, PBS, TRIS, MES, sodium phosphate, and potassium phosphate buffers, and found that PBS and MES buffers are much more benign than the others. We observe a linear dependence of the etch depth over time, and we find the etch rate of silicon dioxide in different buffers that ranges from 2.73 ± 0.76 pm/h in 1 M NaCl to 43.54 ± 2.95 pm/h in $6 \times$ SSC. The protective effects by chemical modifications of the surface are explored. We demonstrate unaccounted glass etching leading to erroneous results with label-free detection of DNA microarrays, and offer remedies to increase the accuracy of quantitative analysis.

1. Introduction

Glass substrates often serve as the solid support in the microarray industry, as they are inexpensive, easy to handle, optically transparent, and expected to be chemically inert. Device miniaturization and immobilization of multiple capture agents on a solid substrate have enabled scientists to study DNA–DNA, DNA–protein, and antibody–antigen interactions in a high-throughput manner (Haab et al., 2001, MacBeath, 2002, Schena et al., 1995, Syvanen, 2001). Furthermore, investigations of various biochemical reactions on microarrays, such as DNA amplification, primer elongation, single base extension and reverse transcription, have emerged (Erdogan et al., 2001, Kinoshita et al., 2007, Mitterer et al., 2004). Whether a biochemical reaction takes places on a solid support or in standard laboratory glassware, it is inevitable that these surfaces will be subjected to the same reaction conditions as the biochemical species of interest. Thus, it is imperative that the surfaces be stable during the entirety of the reaction. For instance, it was shown that a variation of the surface roughness of the glass substrates can contribute to the poor immobilization efficiency of peptide arrays, resulting in a 80% decrease in signal from idealized conditions (North et al., 2010). In addition, unexpected surface inconsistencies can cause artifacts that are not observed in reactions traditionally carried out in solution, leading to an increased number of false positives or false negatives (Sauer et al., 2009).

Silicon dioxide, or more commonly referred as silica or glass, is a very popular choice of material, thanks to its well-known surface chemistry and ease of use in semiconductor micromachining technology. Thus, it is often the choice for sensor surfaces in label-free sensing technologies. While many sensors assume stable glass substrates in their platforms, silica dissolution in even relatively inert solutions with neutral pH has been reported (Icenhower and Dove, 2000, Kato, 1968). Dissolution rates for glass have been reported for time periods ranging from one to a few hundred days; however, there are no studies of silica dissolution during biochemical reactions lasting for several hours to a day. This lack of data for short times is likely due to the fact that quantifying surface etching over such short periods of time is very challenging with conventional methods, such as AFM, which require a vertical resolution better than the surface roughness. Using the Interferometric Reflection Imaging Sensor (IRIS) (Ozkumur et al., 2008), we found that SiO_2 can be etched when the surface is exposed to buffers commonly used in molecular biology protocols. This surface erosion may

* Corresponding author at: College of Engineering, 8 St. Mary's Street, Boston, MA 02215. Tel.: +1 617 353 5067; fax: +1 617 353 6440.
E-mail address: selim@bu.edu (M. Selim Ünlü).

0956-5663/$ - see front matter © 2012 Elsevier B.V. All rights reserved.
http://dx.doi.org/10.1016/j.bios.2012.04.020

compromise data acquired by label-free sensors without the investigator's knowledge, potentially leading to false or inaccurate findings. Because of the inability to measure and quantify small changes on the surface using conventional methods, the phenomenon we present here may have gone unnoticed.

We examined the silica dissolution in multiple buffers at concentrations relevant to biochemical assays. We report, for the first time, the etch rate of thermally grown silicon dioxide in buffers commonly used for microarray research. The etch depth of SiO_2 is measured for various etch times with IRIS, and the effect of the buffer concentration on the etch rate is investigated. The experiments were performed at room temperature, consistent with typical incubation protocols. Our results demonstrate that nearly all buffer solutions we examined etch the silicon oxide surface, in some cases more than 1 nm in 24 h. Because of the relevance to the biosensor field, we investigated whether chemically modified surfaces for biomolecule immobilization suffer from similar dissolution rates as bare silicon oxide surfaces. Furthermore, we explored several immobilization buffers on functionalized silica surfaces to determine their effects on DNA microarray printing. Finally, we offer solutions to the silica etching problem in buffers for quantitative analyses of DNA microarrays.

2. Materials and methods

2.1. Chemicals and buffer preparation

All chemicals were purchased from Sigma-Aldrich unless stated otherwise. Multiple concentrations of sodium phosphate buffer (NaPB) were prepared with monobasic and dibasic sodium phosphate, and the pH was adjusted to 8.5. Potassium phosphate buffer (KPB) was prepared in a similar fashion. Phosphate buffer saline (PBS, Fisher Science) at 10 × was diluted, and saline-sodium citrate (SSC, pH 7.0) and saline-sodium phosphate-EDTA (SSPE, pH 7.4), both 20 × solutions, were diluted to appropriate concentrations. A stock solution of 2-(*N*-morpholino)ethanesulfonic acid (MES) buffer, containing 100 mM MES, 1 M [Na+], and 20 mM EDTA, was diluted to multiple concentrations. Tris(hydroxymethyl)aminomethane (Tris, pH 8.0) buffer were prepared at multiple concentrations, each with 150 mM sodium chloride (NaCl), and different concentrations of NaCl solutions were prepared.

2.2. Substrate preparation and etching experiment

Silicon wafers with 17 μm of thermally grown oxide (Silicon Valley Microelectronics) were protected with photoresist except for repetitive 100 μm circular voids that exposed the silica surface. The samples were immersed in ample amounts of buffer solutions (~15 mL) to avoid any depletion of etching agents for the duration of the experiments: 2, 6, 12, 18, and 24 h. All the experiments took place on a rotating shaker, and the buffer was replaced with a fresh solution after 12 h. Deionized water was used as the negative control. After the etch period, the samples were washed three times in deionized water on the rotator for 10 min, followed by another 5 min wash. The final stage of washing was done by a thorough rinse under a stream of deionized water, after which the samples were dried with ultra pure argon gas. The remaining photoresist was removed by sonicating the samples three times in acetone for 5 min, followed by a acetone, methanol, and deionized water rinse. The samples were dried with nitrogen gas and ashed with O_2 plasma for 10 min (500 W) to ensure the complete removal of any photoresist on the SiO_2 surface. Please refer to the supplementary material for the detail fabrication procedure and the schematic representation of the etching experiment (Fig. S1).

2.3. Interferometric Reflectance Imaging Sensor (IRIS) measurement

The working principle of IRIS is explained in detail elsewhere (Ozkumur et al., 2008). Briefly, a tunable laser is used to illuminate the substrate at 1 nm increments, from 766 nm to 784 nm. The reflected light from the SiO_2 surface and the Si–SiO_2 interface creates an interference signature, and the intensity images at all wavelengths are recorded onto a CCD camera. The data from all of the pixels of the camera are processed to find the optical thickness between the two reflecting surfaces, then translated into a height image of the entire field of view. A simple schematic of the IRIS setup is depicted in the supplementary material (Fig. S2). Using custom software, the relative optical thickness of the etched features was compared to the surrounding background.

2.4. Surface modifications

Silanization The samples were sonicated in acetone for 5 min, rinsed in methanol and deionized water, and dried with argon gas for cleaning. They were then submerged in 10% (w/v) NaOH for 10 min, rinsed with deionized water, and placed in deionized water for 2.5 min on the shaker. After drying with argon, the samples were placed in 3% (v/v) (3-glycidyloxypropyl) trimethoxy silane (epoxy silane, Sigma) in toluene for 3 min followed by a 5 min wash in fresh toluene. Samples were dried with argon gas, baked for 10 min at 100 °C, and stored in a dessicator prior to the experiments.

Polymer coating N,N-dimethylacrylamide (DMA)–acryloyloxy-succinimide (NAS)–3(trimethoxysilyl)-propyl methacrylate (MAPS) (which will be referred as copoly (DMA–NAS–MAPS)) was synthesized as described elsewhere (Cretich et al., 2004) and stored in a dessicator prior to the experiments. Following the same cleaning procedures described in the silanization method, the samples were cleaned with oxygen plasma for 2 min. The samples were then immersed in a 1:1 mixture of 1% (w/v) copoly (DMA–NAS–MAPS) in water and ammonium sulfate at 40% saturation concentration for 30 min, washed thoroughly with deionized water, dried with argon, and baked for 15 min at 80 °C.

2.5. DNA immobilization, hybridization, and denaturation

All of the oligonucleotides were purchased from Integrated DNA Technologies. The detailed sequence information is listed in the supplementary material (Table S1). All oligonucleotides were prepared to 20 μM in various concentrations of NaPB, KPB, and deionized water, and they were spotted with a bench-top robotic spotter (BioOdyssey Calligrapher Miniarrayer, Bio-Rad). For immobilization of duplex DNA, the oligonucleotides were hybridized in 150 mM NaPB prior to spotting. After the spotting was completed, the DNA microarrays were placed in a humidity controlled chamber (65% humidity) overnight to complete the biomolecule immobilization process. The DNA microarrays were washed the following day with the wash protocol that consisted of four times in 2 × SSC for 10 min, twice in 0.2 × SSC for 1 min, and two rinses in 0.1 × SSC prior to imaging.

The DNA microarrays were hybridized with the target oligonucleotide at 1 μM in 3 × SSC buffer in room temperature under constant agitation. Following hybridization, the DNA microarrays were washed with the same wash protocol described above. It was shown that washing in deionized water can denature the duplex DNA on the surface (Daaboul et al., 2011, Ozkumur et al., 2010). For complete denaturation of the duplex DNA, the DNA microarrays were washed three times in deionized water for 10 min each, followed by a thorough rinse in deionized water.

3. Results and discussion

3.1. Etch depth measurements

The samples were masked with photoresist, subjected to multiple buffers at various concentrations for 12 h, and the etch depth was measured with the IRIS following the removal of the photoresist. For each condition, the depth of 40 etched features within the field of view of the IRIS were measured simultaneously and averaged to determine the etch depth. SSC and SSPE buffers are commonly used as the hybridization and wash buffers in DNA or RNA microarray assays, which typically take 2 to 16 h and, in cases, up to a few days to increase the specificity of the reaction. Both buffers removed more than 300 pm of surface silica at room temperature in a 12 h period. MES buffers, which are widely used for hybridization in commercial microarrays, removed less than 150 pm of surface oxide. Buffers commonly used in probe immobilization reactions were also investigated. Multiple concentrations of NaPB and KPB were examined, although 150 mM is the typical concentration in immobilization reactions. The samples in 150 mM of NaPB and 150 mM of KPB were etched >550 pm, and >240 pm, respectively. Buffers commonly used for investigating protein interactions etched much less than the buffers mentioned above. Nevertheless, PBS (probably the most commonly used buffer for any biological reaction in laboratory settings) etched approximately 150 pm of surface silicon oxides. NaCl solutions and TRIS buffers all showed a minimal amount of etching compared to the various citrate and phosphate buffers. The measured etch depths are summarized in the supplementary material (Table S2).

Two controls confirmed our assumption that the measured height differences between the etched features and the protected surfaces are due to the SiO_2 removal. The first control sample was immersed in deionized water and processed and cleaned in parallel with other samples that were exposed to the various buffers. No change in surface height was detected, eliminating concerns that the height difference measurements may be due to any residual photoresist on the surface. The control sample showed a smooth surface after the photoresist removal compared to the distinctive etched patterns created by $6\times$ SSPE buffer as shown in Fig. 1(A). The second control sample was immersed in $6\times$ SSC buffer for approximately 3 days, and the etch depth was measured with the IRIS and with an AFM to ensure that the measured depth is caused by the silica removal rather than a change in optical property of the silicon oxide. The average etch depth of 40 features measured with the IRIS was 1.64 ± 0.02 nm, and the etch depth of a single feature when measured with an AFM was found to be 1.47 ± 0.15 nm, as shown in Fig. 1(B).

3.2. Linearity and concentration dependence of etch rate

The etch depths of the SiO_2 surfaces were measured for various buffer conditions and etch times. Etch depths were found to follow a linear relationship for etch times between 2 h and 24 h for all buffers (Fig. 2(A)). However, for times shorter than 2 h, we found a fairly large *y*-intercept for the linear fit. The slope of the linear fit changes for different concentrations of the same buffer, while the non-zero intercept remains almost constant. The presence of a non-zero intercept was observed before (Kunii et al., 1995). In addition, the etching of thermally grown oxide was reported to show a linear etch rate dependence on the concentration while a comparable non-zero intercept for the linear fit of etch depth versus time was also found (Somashekhar and O'Brien, 1996). Somashekhar and O'Brien suggested that the non-zero intercepts were caused by the continued etching by a thin film of etchants that remain on the surface during the rinse step (Somashekhar and O'Brien, 1996). However, it is difficult to conclude that the continued etching during the washing step could be the exclusive reason for the non-zero intercept, because the maximum amount of rinse time for each sample never exceeded 1 h . Since the purpose of this study was to investigate the etch rate for timescales that are relevant to biochemical processes, the approximately 100 pm of etch for early times (<2 h) was not further investigated.

The etch rates are estimated from the linear fits of etched depth measured at different times, and summarized in Table 1. The etch rate as a function of the concentration of the buffer are plotted in Fig. 2(B), which can be used to estimate the minimum amount of etch when the silicon oxide surface is exposed to PBS and SSC buffers at a particular concentration. One must note that the etching experiments were conducted with constant agitation, as would be the case for biomolecular interaction studies where the system is often well stirred to facilitate mixing. When the surface is exposed to the buffer in a static condition, the etch rate may be much slower (Dove and Crerar, 1990).

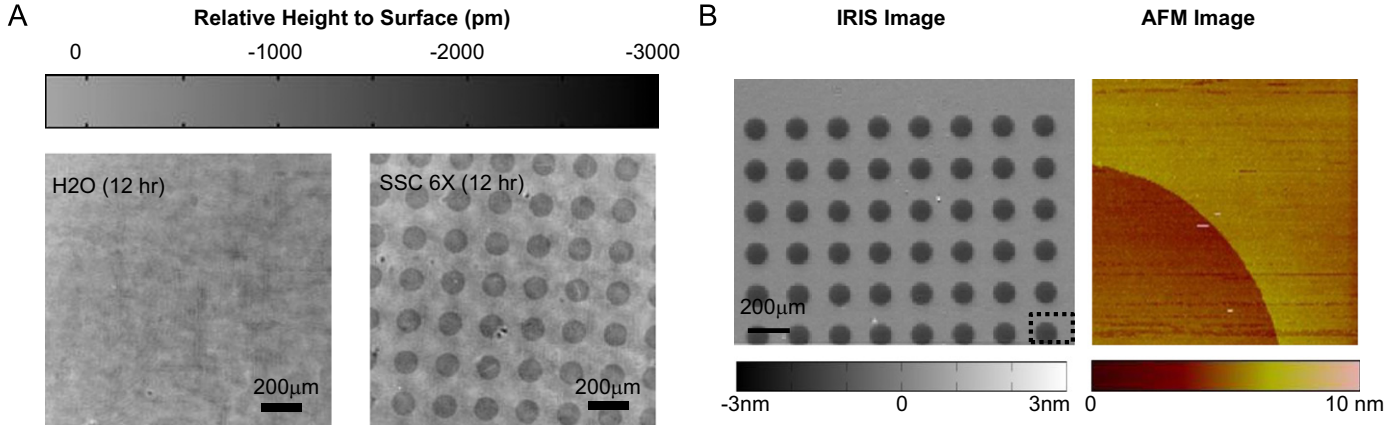

Fig. 1. (A) IRIS images of substrate surfaces. Both samples were protected with photoresist during the experiment. The control sample was in deionized water, and it displays a smooth surface after photoresist removal. The sample left in $6\times$ SSPE buffer for 12 h shows dark areas that correspond to the unprotected regions of the surface. The difference in height of the features compared to the background surface is due to surface SiO_2 removal rather than detection of any remaining photoresist on the surface, as confirmed by the control sample. Negative sign on the reference map represents direction into the surface. (B) An IRIS image and an AFM image of a sample etch with $6\times$ SSC buffer. IRIS measurement of the etch depth was 1.64 ± 0.02 nm when 40 features were averaged. The etch feature inside the dotted box was imaged with the AFM, and the depth was found to be 1.47 ± 0.15 nm.

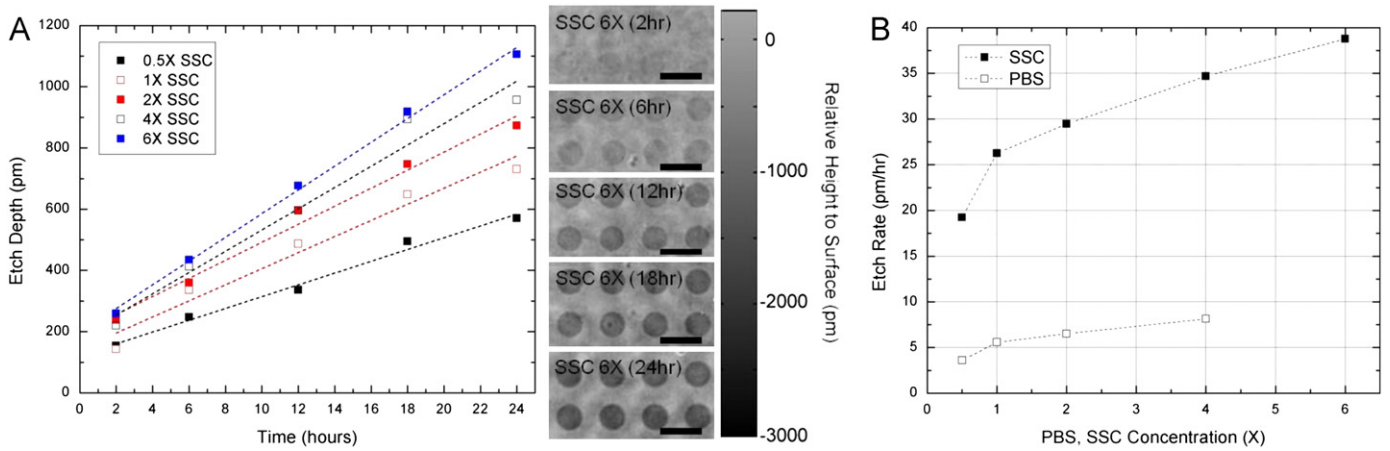

Fig. 2. Measured etch depth in different concentrations of SSC buffer is shown in (A). Each data set displays a linear relation to time with a non-zero intercept. The error bars are not shown for clarity, but are approximately 78 ± 10 pm. Actual IRIS images of the sample surfaces etched in 6 × SSC buffer are shown on the right. The etched areas indicated by darker color become deeper with increasing time. The scale bar on the image is 200 μm. (B) The etch rates vs. concentration. The etch rates of SSC and PBS at different concentrations were found from the linear fits from etch depth with respect to time.

Table 1
Thermally grown silicon oxide etch rate by various buffers. The etch rates were calculated from the linear fits when etch depths was plotted against time. The measured etch depth of the silica in 1 M NaCl, 100 mM MES, and 50 mM TRIS buffers were within the noise level at $t=2$ h and $t=6$ h, and the etch rate in those buffers are not reported.

Solution	Etch rate (pm/h)	R^2
0.5 × PBS	3.69 ± 0.52	0.943
1 × PBS	5.54 ± 1.38	0.835
2 × PBS	6.09 ± 1.33	0.869
4 × PBS	8.12 ± 0.75	0.975
0.5 × SSC	19.28 ± 1.12	0.987
1 × SSC	28.02 ± 3.03	0.955
2 × SSC	30.33 ± 1.92	0.984
4 × SSC	36.54 ± 2.95	0.974
6 × SSC	39.69 ± 1.15	0.997
6 × SSPE	43.54 ± 2.97	0.982
75 mM NaPB	15.15 ± 2.46	0.902
150 mM NaPB	23.25 ± 3.99	0.892
300 mM NaPB	34.09 ± 2.30	0.982
150 mM KPB	12.01 ± 1.43	0.946
600 mM KPB	35.64 ± 2.92	0.974
1 M NaCl	2.73 ± 0.76	0.797

3.3. Quantification of DNA immobilization with various buffers and hybridization

We examined how the surface erosion, caused by different phosphate buffers, affected DNA microarray applications. Oligonucleotides were spotted on copoly (DMA–NAS–MAPS) coated SiO_2 surfaces in the following buffers: 30, 75, 150, 300 mM NaPB (pH 7.5 and pH 8.5), 30, 75, 150, 300 mM KPB (pH 7.5 and pH 8.5), PBS (pH 7.2), and deionized water. 150 mM NaPB (pH 8.5) and 150 mM KPB (pH 8.5) yielded the best probe density (data not shown), and they were chosen to further investigate the error produced due to surface erosion during immobilization. DNA microarrays were prepared with 6 probe types: (1) 5′-NH_2-modified 60mer in NaPB as a negative control; (2) 5′-NH_2-modified 49mer in NaPB; (3) 5′-NH_2-modified 49mer in KPB; (4) 5′-NH_2-modified 49mer in deionized water; (5) non-NH_2-modified 49mer in NaPB; (6) non-NH_2-modified 49mer in KPB. The IRIS images of the microarrays following immobilization is shown in Fig. 3(A) and (B). As expected, there was neither any DNA immobilization nor surface etching where deionized water was used to deposit NH_2-modified oligonucleotides. Both NH_2-modified oligonucleotides (60mer and 49mer) were successfully immobilized with NaPB and KPB on the copoly (DMA–NAS–MAPS) functionalized surfaces, and there was no evidence of immobilization when non NH_2-modified DNA was deposited. No DNA immobilization was observed on the non-functionalized SiO_2 surfaces. It is interesting to note that, while NaPB showed a higher etch rate of SiO_2 than KPB did when the entire sample was immersed in the buffers, NaPB did not affect the surfaces as much when it was deposited with the presence of oligonucleotides on both copoly (DMA–NAS–MAPS) functionalized and non-functionalized silica surfaces.

The DNA microarrays were hybridized with the target that is perfectly complementary to the 5′-NH_2-modified 49mer, and the measured heights of the DNA spots before and after the hybridization are shown in Fig. 3(C) and (D). As expected, there was no height change in the (-)-control spots, and clear hybridization is observed with a large amount of height increase on 5′-NH_2 49mer spots. Molecular surface densities (number of molecules/mm^2) were found based on the measured optical thickness of the DNA spots using a conversion factor of 0.8 ng/mm^2/nm (Ozkumur et al., 2009) and the molecular weights of the corresponding oligonucleotides. The % hybridization was calculated based on the molecular surface densities before and after the hybridization. The apparent % hybridization of the probes immobilized with NaPB showed approximately 92% hybridization, while the probes immobilized with KPB showed 140% hybridization. Hybridization efficiency of over 100% is not possible considering the standard Watson-Crick base pairing of perfectly complementary strands of equal length. If we compensate the initial probe density immobilized with KPB by the amount of etching measured by the etch depth on non-NH_2-modified oligonucleotide spots, the corrected % hybridization becomes 95%. There was no evidence of surface erosion when NaPB was deposited with DNA on copoly (DMA–NAS–MAPS) functionalized silica surfaces. Although a very small amount of etching by NaPB was observed (0.12–0.18 nm) when the same oligonucleotides were deposited on clean SiO_2 surfaces (Fig. 3(D)), it is comparable to the standard deviations of the DNA spots deposited with NaPB (0.15 nm) on the copoly (DMA–NAS–MAPS) coated surface. In addition, one cannot assume that the buffer influences are the same for functionalized and non-functionalized surfaces, as shown in the supplementary material (Fig. S3). Thus, we determined that the surface erosion on a copoly (DMA–NAS–MAPS) functionalized silica surface, caused by NaPB during immobilization, is minimal.

NaPB as a suitable immobilization buffer in a quantitative analysis was further confirmed by comparing the probe density of

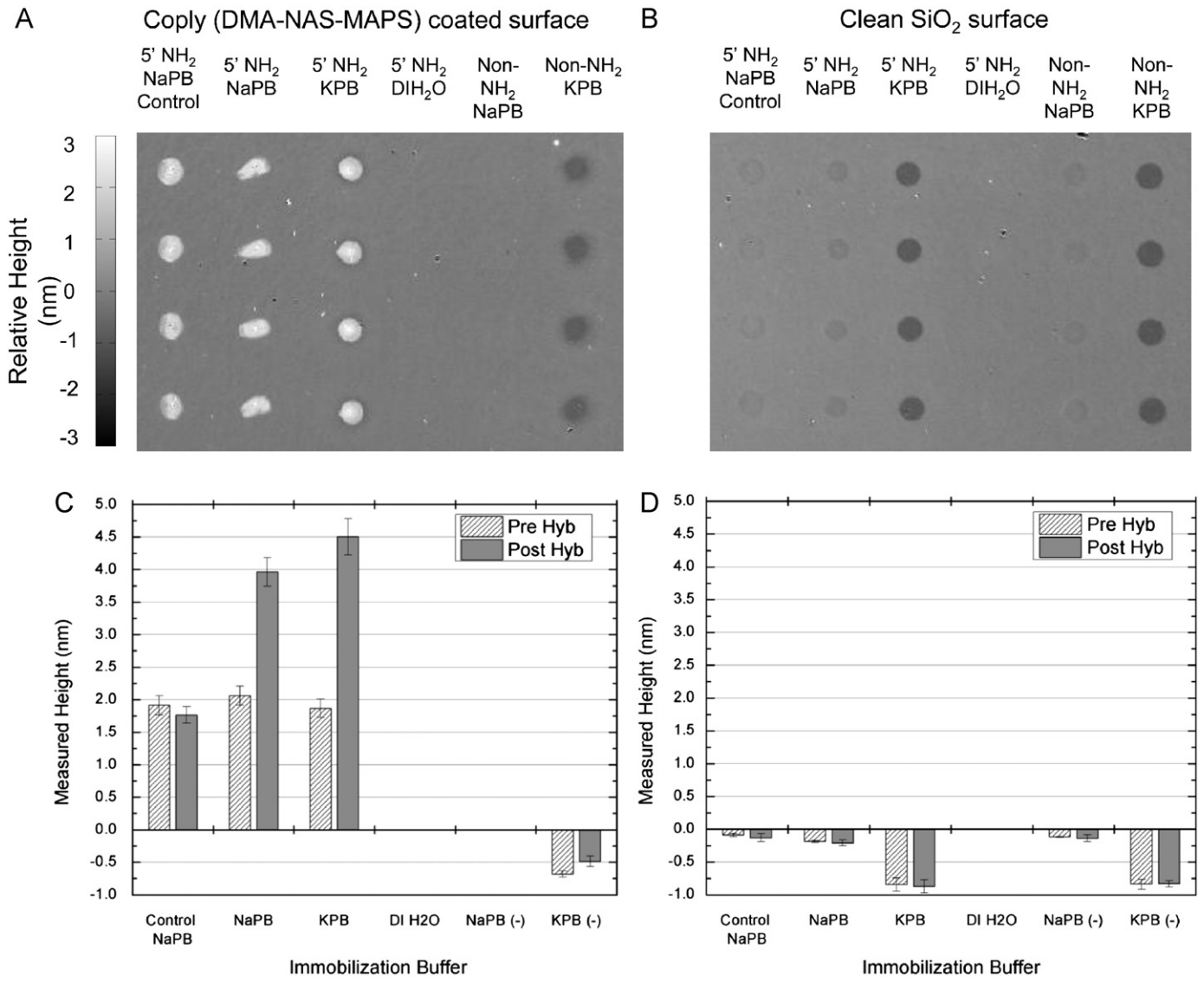

Fig. 3. DNA immobilization and hybridization on a copoly (DMA–NAS–MAPS) functionalized surface and a clean SiO_2 surface. Three different probes (5′ NH_2 modified non-complementary control probe, 5′ NH_2 modified probe, non-NH_2 modified probe) were spotted in 150 mM NaPB, 150 mM KPB, and deionized water (DIH_2O). IRIS images of the DNA microarray on copoly (DMA–NAS–MAPS) functionalized surface is shown in (A), and the same microarray prepared on a clean SiO_2 surface is shown in (B). The measured optical height of the DNA microarray before and after the hybridization is shown in (C)-copoly (DMA–NAS–MAPS) and (D)-clean SiO_2.

dsDNA and its denatured counterpart. The DNA microarrays on copoly (DMA–NAS–MAPS) functionalized surfaces were prepared with the following probes: (1) 18mer ssDNA, (2) 18mer dsDNA, (3) 157mer ssDNA, and (4) 157mer dsDNA. Note that only one strand of the dsDNA had the NH_2 modification for immobilization. Upon immobilization, the microarrays were washed with deionized water to denature the dsDNA. Molecular surface densities were calculated and shown in Fig. 4(A) and (B). The number of molecules on the surface after denaturation remained constant, confirming that any surface erosion caused by NaPB is minimal. It is interesting to note that the immobilization efficiency of dsDNA is much lower than that of ssDNA of the same length. In addition, longer DNA (157mer) showed much lower immobilization efficiency than shorter DNA. One possible explanation for such phenomena can be attributed to the rigidity of dsDNA prohibiting the molecule to penetrate into the 3D polymeric structure (Yalcin et al., 2009). Furthermore, 157mer DNA is larger than the estimated pore size of the copoly (DMA–NAS–MAPS) (Yalcin et al., 2009). The limitation in the penetrability of the rigid dsDNA and longer DNA (157mer) will confine the immobilization to the top surface of the copoly (DMA–NAS–MAPS), and display a similar low immobilization efficiency for longer DNA on a solid surface reported by Steel et al., 2000.

3.4. Stability of DNA microarrays with different surface chemistry

We studied the stability of the immobilized probes on differently functionalized surfaces during hybridization by preparing two DNA microarrays on copoly (DMA–NAS–MAPS) and epoxy silanized silica functionalized surfaces (Fig. 5). The following oligonucleotides were spotted: (1) 5′-NH_2-modified 60mer in NaPB as a negative control; (2) 5′-NH_2-modified 49mer in NaPB. We observed a similar amount of DNA immobilization, and a positive hybridization signal after 2 h of hybridization. The DNA microarrays were then subjected to an additional 36 h of hybridization in 3 × SSC buffer, during which surface silica erosion can have a noticeable effect on the DNA surface density. We found that silane molecules partly protected the silica surface, as

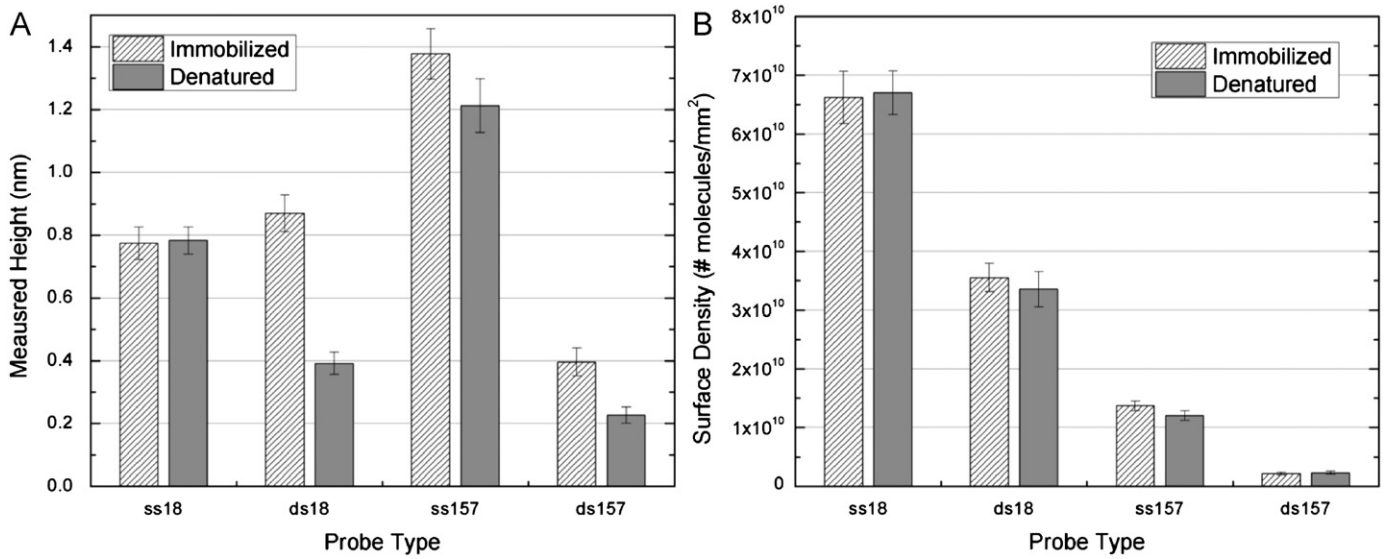

Fig. 4. DNA immobilization and denaturation on copoly (DMA–NAS–MAPS) functionalized surface. Single-stranded and double-stranded DNA were spotted in 150 mM NaPB (pH 8.5) buffer. Based on the optical height measurement with IRIS after immobilization and after denaturation of dsDNA with deionized water (A), the surface density of the oligonucleotides were calculated (B). If there was any surface erosion by NaPB during immobilization, the calculated surface density of the DNA would be smaller for dsDNA after the denaturation. However, the surface density remains constant after denaturation indicating minimal surface erosion during immobilization process.

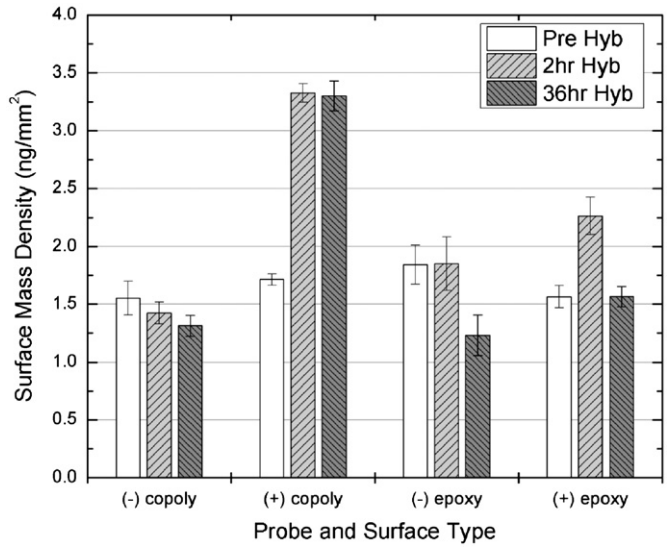

Fig. 5. DNA immobilization and hybridization on copoly (DMA–NAS–MAPS) and epoxy silane functionalized surfaces are shown. For each surfaces, (+) probes, that were complementary to target DNA, and (−) control probes were immobilized. The amount of DNA on the surface was measured with IRIS after immobilization (Pre Hyb), first hybridization (2 h Hyb), and second hybridization (36 h Hyb). $n=20$ for each probe type. The amount of DNA lost after the 36 h hybridization on copoly (DMA–NAS–MAPS) surface is minimal, whereas approximately 0.7 ng/mm^2 of DNA is lost on the epoxy silanized surface.

reported in the supplementary material (Fig. S3); however, we observed much higher probe loss on epoxy silanized surfaces than on the copoly (DMA–NAS–MAPS) functionalized surface. This result is not surprising, considering that the number of anchor points to the surface along the polymeric chain of copoly (DMA–NAS–MAPS) is much smaller than that of a silanized surface. As a result, the loss of immobilized molecules, due to the surface silica erosion, is reduced in the polymer functionalized surfaces relative to silanized surfaces.

4. Discussion

Dissolution of silicon oxides depends on multiple external factors, such as the pH, temperature, presence of electrolytes in the solution, as well as internal factors such as the atomic order of the silicon oxides, and the presence of impurities. Based on the experimental conditions in this study, two possible explanations for the surface erosion mechanisms can be offered. First, hydrolysis of silica in aqueous solutions has been observed and studied extensively (Dove and Crerar, 1990, Dove et al., 2008, Icenhower and Dove, 2000, Oelkers, 2001, Touray and Baillif, 1994) with the following overall reaction:

$$SiO_2\ (s)+2H_2O\ (l)=H_4SiO_4\ (aq)$$

As we report here, raising the concentrations of alkaline cations was reported to increase the dissolution rate of silicon oxides in neutral pH (Dove and Crerar, 1990). Dove et al. suggested that monovalent cations replaced the hydrogen on the surface hydroxide groups, increasing the bond angle and making the surface more accessible to water molecules, which resulted in increased rate of hydrolysis (Dove and Crerar, 1990). Alternatively, phosphate precipitation on the glass surface, followed by a nucleophilic attack by phosphate ions, could cleave the phosphate-silica bond off the surface. This nucleophilic substitution mechanism is similar to that of etching by fluorine ions (Knotter, 2000). In general, phosphate ions in physiological solutions have been shown to facilitate glass dissolution (Baillif and Touray, 1994).

Although the silicon oxide dissolution is a well studied phenomenon, there is no report, to our knowledge, where the silica dissolution or surface erosion is studied in conditions (time scale, pressure, and temperature) relevant to biochemical processes. We found the amount of silica surface etching in commonly used buffers in biochemistry is less than 1 nm during a 12 h period. Etch depths in the sub nanometer range are not trivial to measure with conventional surface profilometers or commercial interferometers (Feng Hua et al., 2004). The surface roughness of approximately 300 pm, as measured with an AFM,

made any measurements of etch depths less than 1 nm very challenging. The IRIS technique is able to resolve such features due to its ability to image a large area and average >300 pixels for a single feature. The noise floor can be further reduced by averaging multiple spots per condition. Thus, we are able to report IRIS measurements on the order of 100 pm for this study because they are well above the reported noise floor of 26 pm (Ozkumur et al., 2008).

Silica dissolution during biochemical processes can pose a serious error in quantitative analyses of biomolecular interactions using label-free sensing platforms, especially when the detection is based on the change in biomolecular mass on the sensor surface. Recently, a significant number of label-free biosensors for protein and DNA arrays have been developed, whose dielectric layer is exposed to buffers investigated in this study (Gauglitz and Proll, 2008, Hwang et al., 2009, Qavi et al., 2009). Optical and mechanical label-free sensors often measure the changes in refractive index, optical path length, or resonant frequencies/wavelengths of the sensors when biomolecule accumulate on the sensor surfaces. Any changes in the dimensions of the sensors due to silica dissolution will likely change the measurements as well as the sensor characteristics leading to erroneous results. For example, whispering gallery mode (WGM) biosensors measures the shift in the resonant wavelengths as biomolecules get captured on the surface, and the wavelength increase is proportional to the radius increase ($\Delta\lambda_r/\lambda_r=\Delta R/R$) (Vollmer and Arnold, 2008). Silica dissolution during the biomolecular interaction will affect WGM devices on two fronts. First, the red-shift in resonant wavelength upon analyte capture is most likely under-represented as the sensor dimension has decreased due to surface silica erosion. Second, surface erosion can affect the evanescent coupling to the optical fibers altering the performance of the sensor. In another example, mechanical sensors, that utilize micro cantilevers to measure the adsorbed mass, are affected as any loss of surface silica will change the mass of the cantilevers. Furthermore, the changed dimension of the cantilever will also alter a number of critical properties such as the spring constant and the resonant frequency of the cantilevers. It is therefore necessary to account for the surface erosion in order to provide accurate quantitative analyses based on the measurements of those sensors. A brief review on various label-free detection techniques and theoretical calculations on the errors introduced by the silica erosion are discussed in the supplementary material.

Interestingly, our results suggest that silica erosion will cause problems to conventional fluorescence-based sensing platforms in addition to label-free sensors. In a typical DNA microarray assay, long hybridization time (>16 h) are recommended to increase the specificity. However, we show that an increase in hybridization times on silanized glass surface reduces the hybridization signal as the surface density of the immobilized probes decreases with the silica dissolution. Phillips et al. addressed the stability of silane chemistry on glass, and offered carbon based surface as an alternative to regular glass surfaces as they presented superior stability (Phillips et al., 2008). Instead of using a more expensive carbon based substrate, we present an alternative surface chemistry of using copoly (DMA–NAS–MAPS) to minimize the immobilized probe loss leading to signal reduction.

5. Conclusion

We quantified the amount of surface silica loss due to etching by commonly used buffers during simulated biological reactions and determined the removal of oxide to be linear with time between 2–24 h. We also determined that increasing the phosphate concentrations and the monovalent cations raised the rate of the surface oxide removal, and that chemical modification provides partial protection of the surface against etching. A correct understanding of this surface modification is particularly important for quantitative detection methods: for example, 100 pm of surface erosion would be equivalent to an erroneous report of 80 pg/mm^2 for DNA and 120 pg/mm^2 for protein desorption from the surface for IRIS measurements (Ozkumur et al., 2009). The error introduced by the surface modification would be further amplified when detecting smaller molecules, as the mass change upon binding becomes comparable to the mass lost by etching.

We make the following suggestions to minimize the error caused by surface erosion in biosensing applications. First, PBS, Tris, and MES buffers are relatively benign and should be considered for protein interactions or DNA hybridizations on a silica surface. Second, polymeric surface chemistries, such as copoly (DMA–NAS–MAPS), are recommended over silane chemistries. Although silane molecules can protect the surface more effectively than the copoly (DMA–NAS–MAPS), there is a higher risk of losing the immobilized molecules when the silica underneath is hydrolyzed. Third, on copoly (DMA–NAS–MAPS) functionalized silica surfaces, we recommend 150mM NaPB (pH 8.5) for DNA immobilization and PBS for protein immobilization, because these buffers permit efficient immobilization while minimizing silica erosion. Finally, the etch rate of silica by the buffers presented in this work must be considered to obtain an accurate quantitative analysis for sensors that utilizes silicon oxide surfaces. The extensive surveying of various buffer effects on silica, and the characterization of the etch behavior on functionalized glass surfaces that we report in this study offer a basis for correction by estimating the biosensor surface erosion. Furthermore, this report raises an important design consideration for biosensor development that was not previously available.

Acknowledgements

We thank Dr. David Freedman for help with the fabrication of the control samples. Funding for this research was provided by Boston University Center for Nanoscience and Nanobiotechnology, and U.S. Army Research Laboratory under Grant W911NF-06-2-0040, and National Science Foundation International Research Experiences for Students grant OISE-0601631.

Appendix A. Supporting information

Supplementary data associated with this article can be found in the online version at http://dx.doi.org/10.1016/j.bios.2012.04.020.

References

Baillif, P., Touray, J.C., 1994. Environmental Health Perspectives. 102, 77–81.
Cretich, M., Pirri, G., Damin, F., Solinas, I., Chiari, M., 2004. Analytical Biochemistry 332 (1), 67–74.
Daaboul, G.G., Vedula, R.S., Ahn, S., Lopez, C.A., Reddington, A., Ozkumur, E., Unlu, M.S., 2011. Biosensors and Bioelectronics 26 (5), 2221–2227.
Dove, P.M., Crerar, D.A., 1990. Geochimica et Cosmochimica Acta 54 (4), 955–969.
Dove, P.M., Han, N., Wallace, A.F., De Yoreo, J.J., 2008. Proceedings of the National Academy of Sciences of the USA 105 (29), 9903–9908.
Erdogan, F., Kirchner, R., Mann, W., Ropers, H.H., Nuber, U.A., 2001. Nucleic Acids Research 29 (7), E36.
Hua, Feng, Anshu Gaur, Y.S., Meitl, Matthew A., Bilhaut, Lise, Rotkina, Lolita, Wang, Jingfeng, Geil, Phil, Shim, Moonsub, Rogers, John A., 2004. Nano Letters 4 (12), 2467–2471.
Gauglitz, G., Proll, G., 2008. Advances in Biochemical Engineering/Biotechnology 109, 395–432.
Haab, B.B., Dunham, M.J., Brown, P.O., 2001. Genome Biology 2, 2.

Hwang, K.S., Lee, S.M., Kim, S.K., Lee, J.H., Kim, T.S., 2009. Annual Review of Analytical Chemistry 2, 77–98.
Icenhower, J.P., Dove, P.M., 2000. Geochimica et Cosmochimica Acta 64 (24), 4193–4203.
Kato K., Y.K., 1968. Journal of the Oceanographical Society of Japan 24 (4), 147–152.
Kinoshita, K., Fujimoto, K., Yakabe, T., Saito, S., Hamaguchi, Y., Kikuchi, T., Nonaka, K., Murata, S., Masuda, D., Takada, W., Funaoka, S., Arai, S., Nakanishi, H., Yokoyama, K., Fujiwara, K., Matsubara, K., 2007. Nucleic Acids Research 35, 1.
Knotter, D.M., 2000. Journal of the American Chemical Society 122 (18), 4345–4351.
Kunii, Y., Nakayama, S., Maeda, M., 1995. Journal of the Electrochemical Society 142 (10), 3510–3513.
MacBeath, G., 2002. Nature Genetics 32, 526–532.
Mitterer, G., Huber, M., Leidinger, E., Kirisits, C., Lubitz, W., Mueller, M.W., Schmidt, W.M., 2004. Journal of Clinical Microbiology 42 (3), 1048–1057.
North, S.H., Lock, E.H., King, T.R., Franek, J.B., Walton, S.G., Taitt, C.R., 2010. Analytical Chemistry 82 (1), 406–412.
Oelkers, E.H., 2001. Geochimica et Cosmochimica Acta 65 (21), 3703–3719.
Ozkumur, E., Ahn, S., Yalcin, A., Lopez, C.A., Cevik, E., Irani, R.J., DeLisi, C., Chiari, M., Unlu, M.S., 2010. Biosensors and Bioelectronics 25 (7), 1789–1795.
Ozkumur, E., Needham, J.W., Bergstein, D.A., Gonzalez, R., Cabodi, M., Gershoni, J.M., Goldberg, B.B., Unlu, M.S., 2008. Proceedings of the National academy of Sciences of the USA 105 (23), 7988–7992.
Ozkumur, E., Yalcin, A., Cretich, M., Lopez, C.A., Bergstein, D.A., Goldberg, B.B., Chiari, M., Unlu, M.S., 2009. Biosensors and Bioelectronics 25 (1), 167–172.
Phillips, M.F., Lockett, M.R., Rodesch, M.J., Shortreed, M.R., Cerrina, F., Smith, L.M., 2008. Nucleic Acids Research 36, 1.
Qavi, A.J., Washburn, A.L., Byeon, J.Y., Bailey, R.C., 2009. Analytical and Bioanalytical Chemistry 394 (1), 121–135.
Sauer, U., Bodrossy, L., Preininger, C., 2009. Analytica Chimica Acta 632 (2), 240–246.
Schena, M., Shalon, D., Davis, R.W., Brown, P.O., 1995. Science 270 (5235), 467–470.
Somashekhar, A., O'Brien, S., 1996. Journal of the Electrochemical Society 143 (9), 2885–2891.
Steel, A.B., Levicky, R.L., Herne, T.M., Tarlov, M.J., 2000. Biophysical Journal 79 (2), 975–981.
Syvanen, A.C., 2001. Nature Reviews Genetics 2 (12), 930–942.
Touray, J.C., Baillif, P., 1994. Environmental Health Perspectives 102, 25–30.
Vollmer, F., Arnold, S., 2008. Nature Methods 5 (7), 591–596.
Yalcin, A., Damin, F., Ozkumur, E., di Carlo, G., Goldberg, B.B., Chiari, M., Unlu, M.S., 2009. Analytical Chemistry 81 (2), 625–630.